Stability and fracture analysis of arch dam based on deformation reinforcement theory

Yuanwei Pan[1,*], Yaoru Liu[1], Qiang Yang[1]

[1] Department of Hydraulic Engineering, Tsinghua University, 100084, China
* Corresponding author: pyw10@mails.tsinghua.edu.cn

Abstract Fracture is a common and significant failure mode of high arch dam. Current theories are still limited in fracture analysis of 3-D structure. In this paper, deformation reinforcement theory (DRT) is deduced and elaborated with a definition of stability that an elasto-plastic structure is stable if equilibrium condition, kinematical admissibility and constitutive equations can simultaneously be satisfied under given external loads. Furthermore, a global stability analysis method of elasto-plastic structure based on DRT is presented. Unbalanced forces can be used to evaluate the stability of structure and indicate fracture initiation and propagation. FEM expression of DRT is deduced and implemented in a three dimensional nonlinear FEM program, and successfully applied in dam heel cracking and multi-crack analysis of arch dam. As statically indeterminate structure, high arch dam is capable of stress redistribution to some extent while cracking occur. This process was expressed in FEM program by iteration and convergence of unbalanced forces. Both elasto-plastic FEM analysis and geo-mechanical experiments are performed on Baihetan and Xiaowan arch dams. Results show that unbalanced forces can be used as the indication of fracture initiation and propagation.

Keywords arch dam, cracks, fracture, stability, unbalanced force

1. Introduction

From the point of view of failure analysis, fracture is a common and significant failure mode of high arch dam, which may result in many problems. In fracture analysis, various factors should be taken into consideration, e.g., material properties, surface notches, cracks, shape and size of structure and working conditions. Those factors present many challenging problems of practical importance range from the micro-scale cavity of materials to macro-scale cracks in engineering structures.

Fracture mechanics has now developed many branches such as linear elastic fracture mechanics (LEFM), nonlinear fracture mechanics, fatigue analysis (e.g., lifetime prediction) and dynamic fracture mechanics. Irwin and Orowan extended Griffith's classical work on brittle materials and proposed both stress and energetic criterions to analyze cracking [1–3], i.e., the stress intensity factor (SIF) and energy release rate, which provided precise measure of fracture toughness and succeeded in predicting cracking behavior. Some significant advances were made by theoretical and experimental mechanics researchers in nonlinear fracture analysis. Wells suggested to assess ductile fracture toughness with crack opening displacement (COD) [4]. Rice proposed J-integral that characterize the intensity of near tip elastic-plastic deformation fields [5]. Besides, numerical methods have developed rapidly, including Finite Element Method (FEM), Discrete Element Method (DEM), Boundary Element Method, eXtended FEM, Numerical Manifold Method and etc.

Those theories mentioned above are based on planar analysis. There is still severe limitation on the applicability of those theories when extended to three-dimension structure. Besides, very little progress has yet been made on understanding the nucleation, growth and interaction of cracks. The description of multi-crack behavior involves complex nonlinear overall deformation, which is beyond the capacity of common numerical methods based on linear plastic.

This paper presents a new approach to deal with cracks in stability and fracture analysis of 3-D structure. Unbalanced force, derived from the Deformation Reinforcement Theory (DRT) [6, 7], could be the criterion of initiation of fracture, the distribution area and magnitude of which could indicate fracture propagation direction [8]. FEM expression of DRT was deduced and implemented

in a three dimensional nonlinear FEM program, and successfully applied in dam heel cracking and multi-crack analysis of arch dam. Both FEM analysis and geo-mechanical experiments are performed on Baihetan and Xiaowan arch dams. Results show that unbalanced forces can be used as the indication of fracture initiation and propagation.

2. Deformation Reinforcement Theory

2.1. Definition of structural stability

Geotechnical structure are characterized by magnificent scale and complicated configurations and working conditions. The classical elasto-plastic theory aims at solving the displacement and stress fields that simultaneously satisfy all the basic equations in boundary value problem, including kinematic admissibility, equilibrium condition and constitutive equations. However, the existence of such solution requires that the structure is stable, i.e., a state where no failure occurs [9]. Structural instability occurs when action is greater than resistance, and the difference between action and resistance defines the unbalanced force. Considering the arbitrary kinematical and equilibrium stress-field, $\boldsymbol{\sigma}_1$, which is termed the trial elastic stress:

$$\boldsymbol{\sigma}_1 = \boldsymbol{\sigma}_0 + \Delta\boldsymbol{\sigma}^{\mathrm{e}} = \boldsymbol{\sigma}_0 + \boldsymbol{D} : \Delta\boldsymbol{\varepsilon} . \tag{1}$$

The kinematical and stable stress-field, $\boldsymbol{\sigma}$, which is the real stress response, could be identified by the following minimization problem:

$$\begin{gathered} \min E\left(\boldsymbol{\sigma}^{yc}\right), \forall f\left(\boldsymbol{\sigma}^{yc}\right) \le 0, \\ E\left(\boldsymbol{\sigma}^{yc}\right) = \frac{1}{2}\left(\boldsymbol{\sigma}_1 - \boldsymbol{\sigma}^{yc}\right) : \boldsymbol{C} : \left(\boldsymbol{\sigma}_1 - \boldsymbol{\sigma}^{yc}\right). \end{gathered} \tag{2}$$

Eq. (2) is known as the closest-point projection method (CPPM) [10], as shown in Fig. 1.

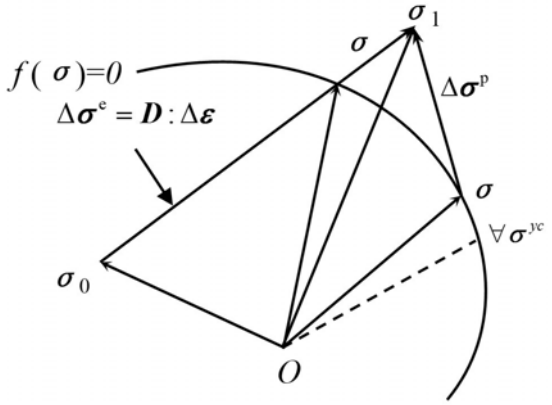

Figure 1. Diagram of elastic-plastic stress adjustment

The difference between $\boldsymbol{\sigma}_1$ and $\boldsymbol{\sigma}$ is the plastic-stress increment field $\Delta\boldsymbol{\sigma}^{\mathrm{p}}$:

$$\Delta\boldsymbol{\sigma}^{\mathrm{p}} = \boldsymbol{\sigma}_1 - \boldsymbol{\sigma} . \tag{3}$$

The plastic-stress increment field $\Delta\boldsymbol{\sigma}^{\mathrm{p}}$ leads to the plastic-strain increment field $\Delta\boldsymbol{\varepsilon}^{\mathrm{p}} = \boldsymbol{C} : \Delta\boldsymbol{\sigma}^{\mathrm{p}}$, while $\boldsymbol{C}$ is the fourth-order compliance tensors.

Clearly, the minimization variable $\boldsymbol{\sigma}$ restricted by the yield criterion can be viewed as the material resistance while the minimization objective $\boldsymbol{E}$ in Eq. (2), termed the volume density of the plastic complementary energy (PCE), represents the difference between the plastic dissipations of the stress action and the material resistance,

$$E\left(\boldsymbol{\sigma}\right) = \frac{1}{2}\left(\boldsymbol{\sigma}_1 - \boldsymbol{\sigma}\right) : \boldsymbol{C} : \left(\boldsymbol{\sigma}_1 - \boldsymbol{\sigma}\right). \tag{4}$$

Thus, stability of a material point can be interpreted as the condition that the stress action is greater

than the material resistance in the sense of plastic dissipation: $E(\boldsymbol{\sigma}) > 0$. Furthermore, stability of a structure whose volume is V can be deduced as

$$\Delta E = \frac{1}{2}\int_V \Delta\boldsymbol{\sigma}^{\mathrm{p}} : \boldsymbol{C} : \Delta\boldsymbol{\sigma}^{\mathrm{p}} \mathrm{d}V . \tag{5}$$

This equation shows that ΔE is also the norm of plastic-stress increment field $\Delta\boldsymbol{\sigma}^{\mathrm{p}}$. If $\Delta E = 0$, then $\Delta\boldsymbol{\sigma}^{\mathrm{p}}$ is always zero and the structure is stable. If $\Delta E > 0$, the structure is unstable.

2.2. Expression in FE analysis

In this section, DRT is deduced and implemented in elasto-plastic FE analysis. For simplicity, the problem is restricted in displacement method, which means the kinematic admissibility is naturally satisfied.

Since $\boldsymbol{\sigma}_1$ is a equilibrium stress-field, it satisfies equilibrium condition:

$$\boldsymbol{F} = \sum_e \int_{Ve} \boldsymbol{B}^{\mathrm{T}} \boldsymbol{\sigma}_1 \mathrm{d}V . \tag{6}$$

$\boldsymbol{F}$ is equivalent nodal force vector of external loads. $\boldsymbol{B}$ denotes the displacement gradient matrix.

Applied with Eq. (3) and after simple manipulations, Eq. (6) can be recast into the following expression:

$$\Delta\boldsymbol{U} = \sum_e \int_{Ve} \boldsymbol{B}^{\mathrm{T}} \Delta\boldsymbol{\sigma}^{\mathrm{p}} \mathrm{d}V = \sum_e \int_{Ve} \boldsymbol{B}^{\mathrm{T}} (\boldsymbol{\sigma}_1 - \boldsymbol{\sigma}) \mathrm{d}V = \boldsymbol{F} - \sum_e \int_{Ve} \boldsymbol{B}^{\mathrm{T}} \boldsymbol{\sigma} \mathrm{d}V . \tag{7}$$

$\Delta\boldsymbol{U}$ is the driving force of the deformation process that can be termed the unbalanced force. It's also referred to as the residual force in FEM, which is a set of equivalent nodal forces of the difference between the two stress fields $\boldsymbol{\sigma}_1$ and $\boldsymbol{\sigma}$.

2.3. Fracture analysis based on DRT

Liu Y. R. et al. proved both theoretically and experimentally that the unbalanced force can be used as the prediction and measurement of failure mechanism [8]. Failure occurs where there is unbalanced force subjected to prescribed loads, and the structure is unstable in the sense of PCE. So the unbalanced force can be used to evaluate fracturing of structure.

According to DRT, unbalanced forces are the driving force of structural failure, and fracture is part of the failure mechanism. Thus, unbalanced forces could be the determination of fracture location. The area where unbalanced forces occur is the location where the fracture initiates. Furthermore, the amount of unbalanced force incurred by external load represents the extent of fracture propagation. The development of unbalanced forces is the process of propagation of the fracture.

3. Application in high arch dam

In this section, unbalanced forces are applied to indicate initiation of dam heel cracking, and to verify the dominating cracks from multi-crack arch dam.

3.1. Dam heel cracking analysis of Baihetan arch dam

Baihetan arch dam, located in an asymmetrical "V"-shaped valley, is 289 m high. Both 3-D finite element numerical and geo-mechanical experiments are performed. The finite element mesh model is shown in Fig. 2(a). Various rock materials and faults are simulated. The size of FE model is as follows:

Upper stream: 1.5 times of the height of dam (500 m);

Down stream: 2.5 times of the height of dam (700 m);
Left and right banks: 3 times of the height of dam (800 m each);
Height above the dam: 50 m;
Height beneath the dam: 324 m.
Fig. 2(b) is photo of the arch dam model and distribution of devices. The geo-mechanical model is built in a steel frame whose size is 4.6 m×4.6m×2.8 m. The model scale is 1:250.

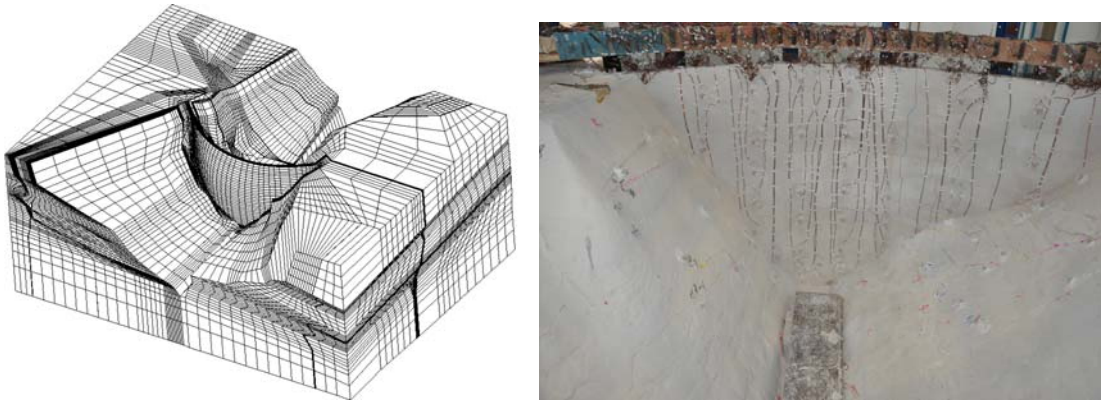

(a) Numerical mesh (b) geo-mechanical model
Figure 2. Numerical mesh and geo-mechanical model of Baihetan arch dam

Fig. 3 shows that unbalanced forces of upstream surface concentrate near the foundation plane, especially the dam heel near river bed area. Unbalanced forces distribution contour of dam heel in different work conditions are shown in Fig. 4. The unbalanced forces concentrated in the upstream river bed area near the dam heel instead of the dam itself, where there is a fault crossing. Unbalanced forces form a significant banding in this area, which is termed as the indication of cracks initiation.
Cracking status of the dam heel near river bed area during the geo-mechanical test are illustrated in Fig. 5. When work load reaches 1.5 times water pressure, micro-cracks initiate in the upstream river bed about 14.5 m away from dam heel, which agrees with the FE analysis results. Cracks propagate as work load increases to 2.0 times water pressure, and begin to penetrate through the river bed.

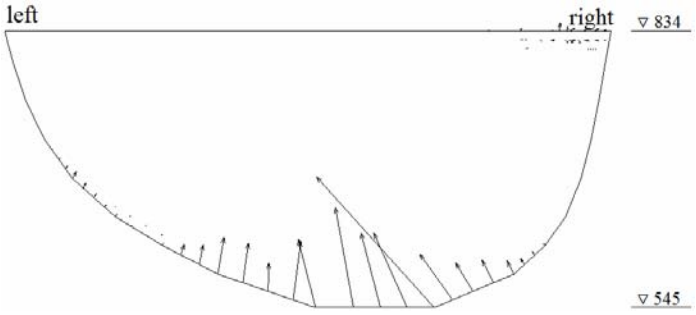

Figure 3. Unbalanced forces distribution of upstream surface

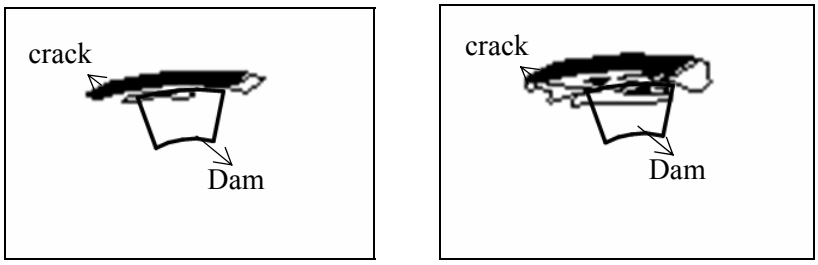

(a) 1.5 times water pressure (b) 2.0 times water pressure
Figure 4. Unbalanced forces distribution of dam heel

(a) 1.5 times water pressure (b) 2.0 times water pressure

Figure 5. Cracking status of the dam heel near river bed area

3.2. Fracture analysis of Xiaowan arch dam

Xiaowan arch dam is subjected to numerous cracks due to the temperature control program. In the following example, we simulate the major cracks in the dam and analyze parameters sensitivity with DRT method. Results and conclusions of geo-mechanical model test are also given as comparison with numerical method.

FE computation model of Xiaowan includes 58989 nodes and 53850 elements, while 11 cracks in the dam are simulated with thin layer elements, as shown in Fig. 6. Since engineering measures have been applied, the parameters of crack elements are as follows: E=5GPa, μ=0.3, γ=27.5kN/m^3, f=1.12, c=0.9MPa. Parameters E, f, c are reduced with certain percentages in five schemes, respectively 100% (scheme 1), 50% (scheme 2), 30% (scheme 3), 10% (scheme 4) and 5% (scheme 5). Both normal and overload conditions are included in each scheme. Unbalanced forces of cracks and dam heel in scheme 1 and 3 are given by Table 1 and Table 2.

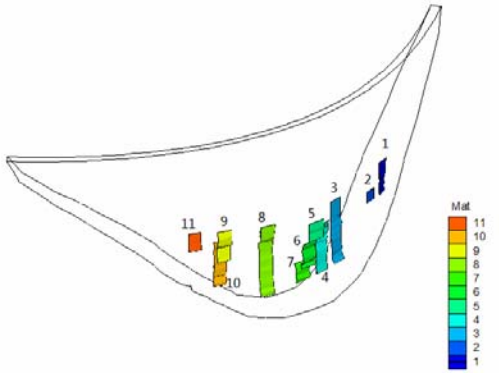

Figure 6. Distribution of cracks in Xiaowan arch dam

Table 1. Unbalanced forces of cracks and dam heel in scheme 1 (10^4 N)

No.	Crack	Dam weight	Water pressure	1.5 times water pressure	2 times water pressure	2.5 times water pressure
1	13lf-1	0.06	0.00	0.36	1.36	32.50
2	13lf-2	0.01	0.00	1.23	4.84	76.41
3	20lf-1	0.02	0.00	0.00	0.00	13.92
4	20lf-2	0.00	0.00	0.58	6.63	11.95
5	22lf-1	0.00	0.00	0.00	0.00	0.00
6	22lf-3	0.00	0.00	0.00	0.00	0.00
7	22lf-4	0.00	0.00	0.00	0.00	0.00
8	25lf-1	0.00	0.00	0.00	0.00	1.04
9	28lf-1	0.01	0.00	0.00	0.00	3.99
10	28lf-2	0.05	0.00	1.91	13.10	24.79
11	30lf-1	0.00	0.01	0.41	16.73	29.77
Dam heel		4122.63	40249.56	257289.9	415601.5	561660.5

* Crack 13lf-1 in the table means the first crack in No. 13 dam section, and so on.

Table 2. Unbalanced forces of cracks and dam heel in scheme 3 (10^4 N)

No.	Crack	Dam weight	Water pressure	1.5 times water pressure	2 times water pressure	2.5 times water pressure
1	13lf-1	0.11	0.88	1.59	3.11	38.11
2	13lf-2	0.04	1.98	25.22	67.44	92.83
3	20lf-1	0.13	0.00	0.00	0.00	14.30
4	20lf-2	0.00	18.05	597.84	1902.98	3216.86
5	22lf-1	0.00	0.00	0.00	0.00	0.00
6	22lf-3	0.06	0.00	0.00	0.00	0.00
7	22lf-4	0.00	0.00	0.00	0.00	0.00
8	25lf-1	0.25	0.00	0.00	0.00	0.47
9	28lf-1	155.71	0.00	0.95	20.05	110.01
10	28lf-2	0.65	18.39	2321.18	9522.02	18778.98
11	30lf-1	69.33	0.19	29.91	124.81	897.03
Dam heel		4005.15	40225.05	257428.3	415430.9	561604.5

Table 1 and Table 2 show that unbalanced forces of dam heel increase earlier than cracks in the dam. Dam heel contributes the major unbalanced forces in all condition. Namely, dam heel cracking occurs before any crack propagates. Among all existing cracks, 20lf-2 and 28lf-2 are the dominating cracks in the process of fracture propagation.

The final crack status of upstream dam surface in geo-mechanical model test is shown in Fig. 7. In normal working condition, dam cracks are mostly in compression-shear state, and neither yielding nor tension fracture is involved. Dam heel cracking occurs as the work load increases to 1.7~3.0 times normal pressure. There is no sign of crack propagation in the dam during the test. Instead, cracks that occur on the dam surface begin to extend after the work load reaches 4.0 times normal pressure. Experimental results indicate that dam heel cracking, compared with dam cracks, is the dominating problem of Xiaowan arch dam, which is corresponding to FEM results.

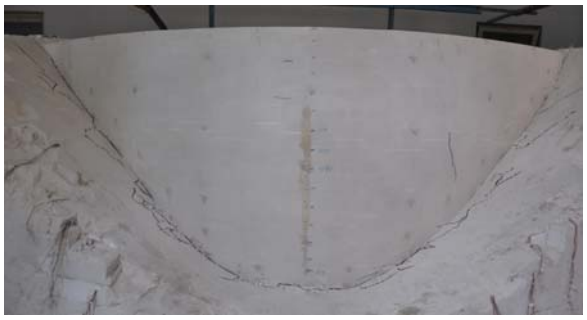

Figure 7. The final crack status of upstream dam surface

4. Conclusions

This paper presents a new approach to deal with cracks in stability and fracture analysis of 3-D structure. Unbalanced force, derived from the Deformation Reinforcement Theory (DRT), could be the criterion of initiation of fracture, the distribution area and magnitude of which could indicate fracture propagation direction. FEM expression of DRT is deduced and implemented in a three dimensional nonlinear FEM program, and successfully applied in dam heel cracking and multi-crack analysis of arch dam. Both elasto-plastic FEM analysis and geo-mechanical experiments are performed on Baihetan and Xiaowan arch dams. Dam heel cracking and multi-crack propagation analysis are presented. Results of geo-mechanical experiments show great agreement with FEM analysis. Unbalanced forces can be used as the indication of fracture initiation and propagation.

Acknowledgements

The work reported here was supported by State key Laboratory of Hydroscience and Hydraulic Engineering under grant No. 2013-KY-2 and China National Funds for Distinguished Young Scientists under grant No. 50925931.

References

[1] G. R. Irwin, Fracture dynamics, in: Fracturing of metals. Cleveland: Am. Soc. Metals, 1948. 147–166.
[2] E. Orowan, Fracture and strength of solids, in: Rep. on Progr. in Phys., 1948. 185.
[3] G. R. Irwin, Analysis of stresses and strains near the end of a crack transversing a plate. J. Appl. Mech., 24 (1957) 361–364.
[4] A. A. Wells, Application of fracture mechanics at and beyond general yielding. British Welding J, 10 (1963) 563–570.
[5] J. R. Rice, A path independent integral and the approximate analysis of strain concentration by notches and cracks, Journal of Applied Mechanics, 35 (1968) 379-386.
[6] Yang Q., Liu Y. R., Chen Y. R., Zhou W. Y., Deformation reinforcement theory and global stability and reinforcement of high arch dams. Chin J Rock Mech Eng, 6 (2008) 1121–1136.
[7] Yang Q., Chen X., Zhou W. Y., Yang R. Q., On unbalanced forces in 3D elastoplastic finite element analysis. Chin J Geotech Eng, 3 (2004) 323–326.
[8] Liu Y. R., Chang Q., Yang Q., WANG C. Q., GUAN F. H., Fracture analysis of rock mass based on 3-D nonlinear Finite Element Method. Sci China Tech Sci, 54 (2011) 556–564.
[9] Yang Q., Leng K. D., Chang Q., Liu Y. R., Failure mechanism and control of geotechnical structures. Yang Q., et al. (Eds.), Constitutive Modeling of Geomaterials, Springer Berlin Heidelberg, 2013, pp. 63-87.
[10] Simo, J. C., Kennedy, J. G., Govindjee, S., Non-smooth multisurface plasticity and viscoplasticity, Loading/unloading conditions and numerical algorithms. Int. J. Numer. Methods Engrg. 26 (1988) 2161–2185.